Int. J. Electrochem. Sci., 9 **(2014)** 8097 - 8105

International Journal of
ELECTROCHEMICAL
SCIENCE
www.electrochemsci.org

Short Communication

Hydrogen Evolution in the Presence of CO_2 in an Aqueous Solution during Electrochemical Reduction

Yangchun Lan[1,2], *Sichao Ma*[3], *Paul J.A. Kenis*[2,*], *Jiaxing Lu*[1,*]

[1] Key Laboratory of Green Chemistry and Chemical Processes, Department of Chemistry, East China Normal University, Shanghai 200062, PR China.
[2] Department of Chemical and Biomolecular Engineering, University of Illinois at Urbana-Champaign, Urbana, IL 61801, USA.
[3] School of Chemical Sciences, University of Illinois at Urbana-Champaign, Urbana, IL 61801, USA.
[*]E-mail: kenis@illinois.edu; jxlu@chem.ecnu.edu.cn

Received: 27 August 2014 / *Accepted:* 19 September 2014 / *Published:* 28 October 2014

This study investigated the electroanalytic behaviors of different Cu(core)/CuO(shell) catalyst loadings in a standard three-electrode cell in an aqueous solution. Transformations between Cu, Cu(I), and CuO as a function of applied potential were observed. Electrochemical reduction in the presence of CO_2 was conducted in a flow reactor. Hydrogen evolution occurred during electrochemical reaction. The H_2 Faradaic efficiency was between 40% and 65%. Differential equations were used to model the hydrogen evolution reaction. The models were able to describe the electrochemical reduction that occurred. According to kinetic analysis, the H_2 rate constant was not affected by increased catalyst loadings.

Keywords: hydrogen evolution, electrochemical reduction, Cu(core)/CuO(shell) nanopowder, catalysis, aqueous solution, CO_2

1. INTRODUCTION

Growing global energy demands and depletion of fossil-fuel reserves have prompted extensive research on alternative energy conversion and storage systems that exhibit high efficiency, low cost, and environmental benignity [1-3]. There was considerable interest in H_2 because it was the cleanest energy vector. H_2 can solve urban pollution problems because H_2 fuel cells can power electric motors in zero-emission vehicles [4]. Although H_2O electrolysis is an expensive technique because of its high energy consumption, this process produces hydrogen [5-7].

Large-scale consumption of fossil fuels has increased atmospheric carbon dioxide (CO_2) levels over the past 100 years; as of date, the CO_2 value is 400 ppm and is still increasing [8]. High atmospheric CO_2 concentrations have caused severe environmental problems, such as climate change [9, 10]. CO_2 reduction would not only solve environmental problems, but it would also cause economic gains because this reaction produces substances that include carbon oxide, formic acid, methanol, and hydrocarbons (HC) [11-14]. Electrochemical reduction of CO_2 in an aqueous solution has gained considerable interest because it is a potential method for producing valuable chemicals [15, 16]. Hydrogen evolution reaction (HER) occurs together with CO_2 reduction during electrochemical reaction in an aqueous solution. Some researchers modified catalysts or used high H_2 over-potential electrode to suppress H_2 production [17, 18]. Therefore, aside from obtaining the necessary intermediates, H_2 is also produced during CO_2 electrochemical reduction in an aqueous solution. This process is an effective method to convert CO_2 and produce H_2 [19].

The use of a copper (Cu) electrode has attracted considerable attention because of its ability to produce HC products at reasonable currents and efficiencies [12, 17, 20-24]. In several industries, the widespread use of Cu-based catalysts in producing chemicals from CO_2 reduction was observed [25, 26]. Previous studies showed that copper oxides adsorbed protons during CO_2 electrochemical reaction or photoreduction in an aqueous solution, causing HER [27-30]. However, only a few studies on the electrochemical reduction of CO_2 that used a metal core/metal oxide shell-structured catalyst have been conducted. In this study, we investigated the electrochemical reduction of CO_2 in a flow reactor containing 1 M $KHCO_3$ in the presence of the Cu (core)/CuO (shell) catalyst. The catalyst predominantly produced CO and HCOOH, and H_2 was its byproduct. The CO_2 reduction's Faradaic efficiency was between 10% and 45%, which was lower than that of H_2. Furthermore, we performed a detailed investigation of the H_2 evolution that occurred in a flow reactor; the process was conducted in the presence of CO_2 using the Cu(core)/CuO(shell) catalyst in an aqueous solution.

2. EXPERIMENTAL SECTIONS

Cu(core)/CuO(shell) nanopowder (APS of 20 nm to 40 nm, 99.9%, metal basis, Alfa Aesar) inks were prepared by mixing Millipore water (200 μL), catalyst (4 mg), Nafion® solution (5.2 μL, 5 wt%, Fuel Cell Earth), and isopropyl alcohol (200 μL, 99.9%, Fisher Scientific). The inks were then sonicated (Vibra-Cell ultrasonic processor, Sonics & Materials, Inc.) for 15 min and then hand-painted on a microporous layer of Sigracet 35 BC gas-diffusion layer (Ion Power, Inc.). All cathodes in the flow reactor were loaded with either 0.5, 1.0, 1.5, or 2.0 mg/cm^2 of the Cu(core)/CuO(shell) catalyst on a Sigracet 35 BC. However, all the anodes (high-surface area platinum (Pt) black, Alfa Aesar) used in the flow reactor were loaded with 1 mg/cm^2 of the Cu(core)/CuO(shell) catalyst on a Sigracet 35 BC.

Electroanalytical experiments (autolab potentiostat, PGSTAT-302N, EcoChemie) were conducted in 1 M $KHCO_3$ (granular, ACS reagent, 99.7%, Sigma Aldrich). A standard three-electrode electrochemical cell equipped with a glassy carbon electrode was used as the working electrode. A Pt gauze and an Ag/AgCl in 3 M NaCl were used as the counter and reference electrodes, respectively. All experiments were performed at room temperature under atmospheric pressure. The catalyst inks

were prepared using the same method described above. The catalyst layer for the three-electrode cell experiments was prepared as follows: around 5 μL of the catalyst ink was deposited and dried under flowing N_2 on a glassy carbon rotating-disk electrode (Metrohm 6.1204.300) that was polished using 0.05 micron alumina.

Electrolysis in the flow reactor was operated at room temperature under atmospheric pressure [31-33]. A Nafion-117 membrane was used to separate the cathode and the anode compartments to prevent the oxidation of reduced CO_2 products. An autolab potentiostat (Autolab PGSTAT-302N, EcoChemie) that was operated on chronoamperometric mode was used to measure the resulting currents, as previously reported [34]. Individual electrode potentials were measured using multimeters that were connected to each electrode and a Ag/AgCl reference electrode in the exit stream. A mass flow controller (MASS-FLO, MKS instrument) was used to maintain the CO_2 flow at 7 sccm from a cylinder. 1 M $KHCO_3$ was injected in the flow reactor at 0.5 mL/min using a syringe pump (PHD 2000, Harvard Apparatus). The H_2 composition was analyzed by allowing the effluent gas stream to flow directly in a gas chromatograph (GC; Thermo Finnegan Trace GC). The GC was operated in thermal conductivity detection (TCD) mode. Carboxen-1000 (Supelco) was the column used and the He carrier gas was set at a flow rate of 20 sccm. The column temperature was 150 °C and the TCD detector's temperature was 200 °C [35, 36].

3. RESULTS AND DISCUSSION

3.1 Cyclic voltammetry

The electrochemical behavior of different Cu(core)/CuO(shell) catalyst loadings were studied in detail using two successive scans. As evident in Figure 1**(**a1) and **1**(a2), a reductive peak at –1.1 V [peak I in Figure 1(a1)] was observed after bubbling argon (Ar) in the first scan. Two small successive oxidative peaks were observed at –0.12 V and +0.11 V in the reverse scan; these peaks were also present in the second scan. The two oxidative peaks were described as the oxidation of Cu to Cu(I) and Cu(I) to Cu(II), respectively; this result was in agreement with results of a previous study [37]. However, peak I in the first scan was not present in the second scan, and two reductive peaks were observed at –0.22 V and –0.62 V [III and IV, respectively in Figure 1(a2)]. These two peaks represented the transition of Cu(II) to Cu(I) and Cu(I) to Cu, respectively. Therefore, the reductive peak in the first scan was caused by the combination of reduced CuO(shell) to Cu. Peak current increased with increasing catalyst loadings. In the scan range from –1.0 V to –1.5 V, the polarized curve was not observed in the first scan [Figure 1(b1)], which overlapped with the catalyst reduction peak. However, the onset potential of the polarized curve in the second scan became more positive with increasing catalyst loadings [Figure 1(b2)]. We speculated that more protons were absorbed on the electrode surface with increasing catalyst loadings, which was favorable for HER. The electroanalytic behavior (in CO_2 atmosphere) and the cyclic voltammetry (in Ar atmosphere) of the different catalyst loadings were similar, except that some of the peaks shifted and an increase in current was observed in the cyclic voltammetry results. This behavior was due to the reduction of CO_2

on the catalyst surface or the reaction of CO_2 and a proton. At a scan range from –1.0 V to –1.5 V in the presence of CO_2 [Figure 1(c1) and 1(c2)], the onset potential of the polarized curve became more positive with increased catalyst loadings.

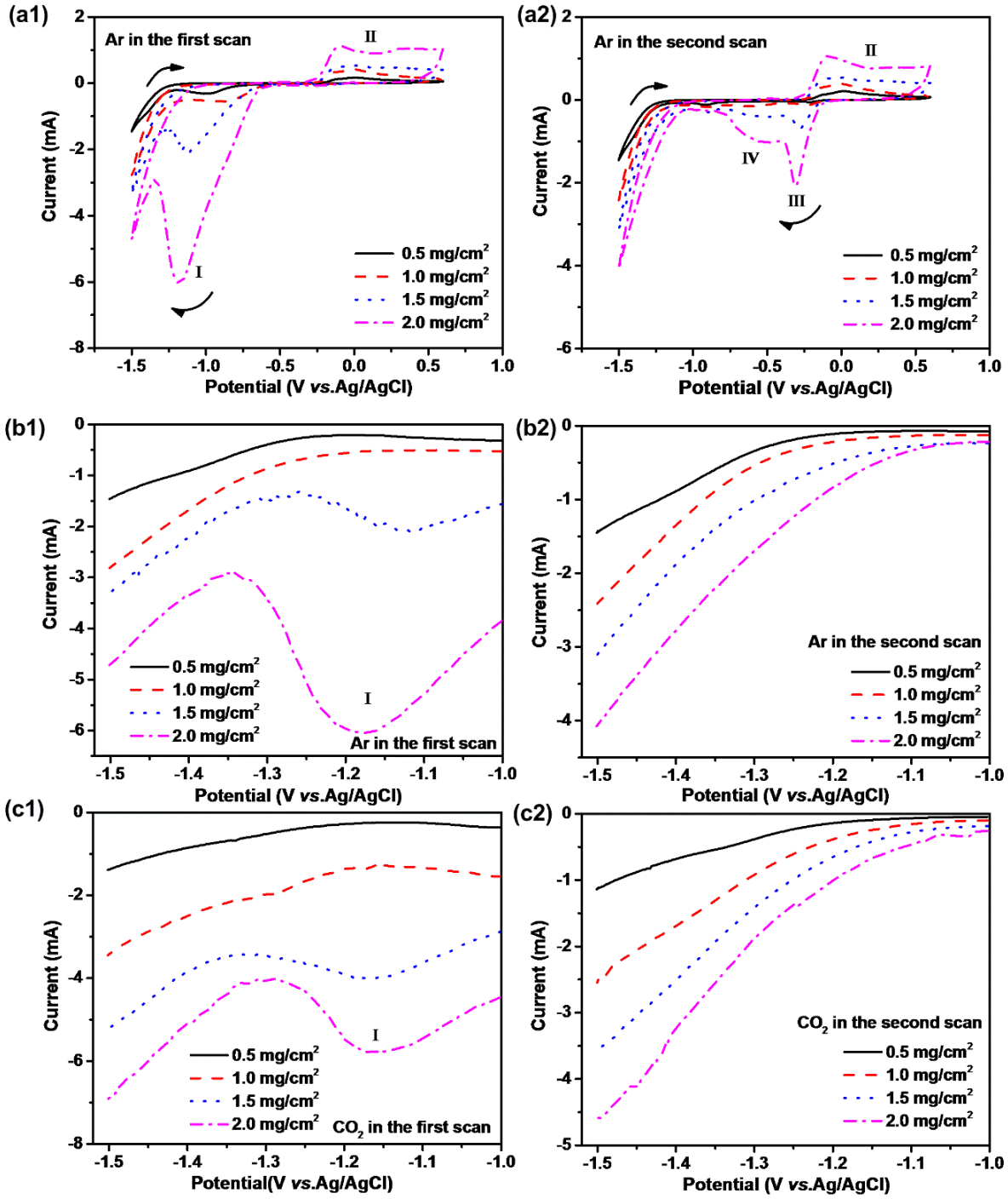

Figure 1 Cyclic voltammograms of different Cu(core)/CuO(shell) loadings in 1 M $KHCO_3$ in the presence of Ar and CO_2. Sweep rate was 0.1 V/s. (a1) and (a2) were the electroanalytic behaviors of catalyst in the first and second scan, respectively; the reduction scan of catalyst in the small range were shown from b1 to c2, respectively.

3.2 Electrolysis

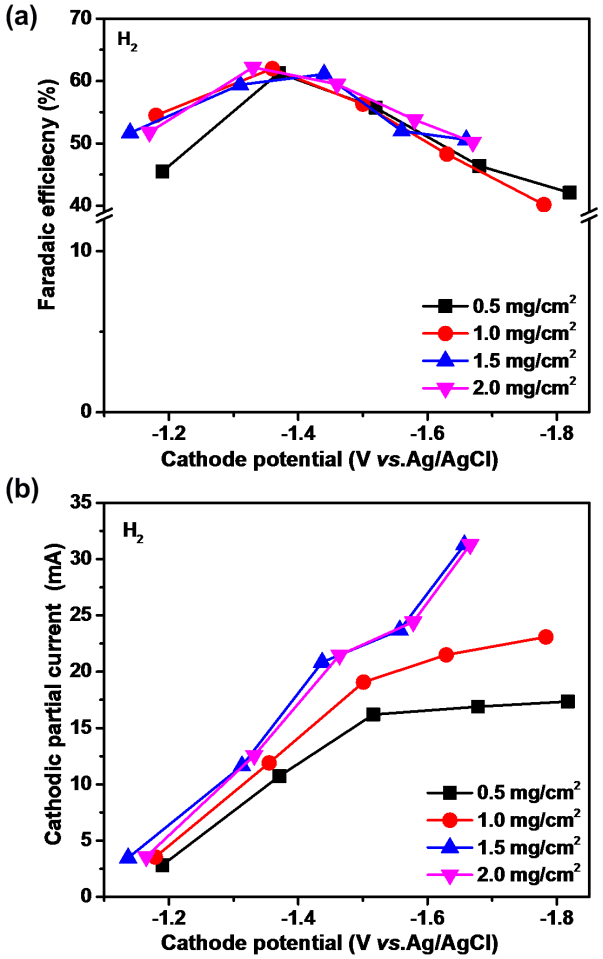

Figure 2. Faradaic efficiency and cathodic partial current of products on different loadings Cu(core)/CuO(shell) (a) and (b) in 1 M $KHCO_3$ in a flow reactor.

Chronoamperometric electrolysis was performed in a divided flow reactor equipped with gas - diffusion electrodes (GDEs) in the presence of CO_2. This process was performed to understand the effect of different Cu(core)/CuO(shell) catalyst loadings on the electro-reduction reaction in 1 M $KHCO_3$. The experimental results are shown in Figure 2. CO and HCOOH were the predominant CO_2 reduction products and H_2 was the byproduct during the electrochemical reaction in an aqueous solution. Faradaic efficiencies of CO and HCOOH were between 10% and 45%. This study focused more on HER [Figure 2(a)], at the cathode potential from -1.1 V to – 1.82 V vs.Ag/AgCl, Faradaic efficiency were between 40% and 65%. While using copper as electrode, Faradaic efficiency of H_2 was 20.5% at -1.44 V *vs*.NHE (so -2.051 V *vs*.Ag/AgCl) [17]. In this work, using Cu(core)/CuO(shell) as catalysis, copper oxides easily adsorbed protons [27-30], which was favor for HER. The H_2 Faradaic efficiency initially increased and then decreased when the cathode potentials shifted to more negative values. At –1.78 V vs.Ag/AgCl and when catalyst loading was 1.0 mg/cm^2, the H_2 Faradic efficiency

decreased to 40%. When catalyst loadings were 1.5 and 2.0 mg/cm^2, the H_2 Faradaic efficiency was higher than that of the other catalyst loadings. This behavior was attributed to the increase in catalyst loading, causing more protons to adsorb on the GDE surface. This result was consistent with cyclic voltammetry results [Figure 1(c2)]. The H_2 Faradaic efficiency was not affected by increases in catalyst loading.

Cathodic partial current was produced by multiplying the current at a given potential the Faradaic efficiency. The effect of catalyst loadings on the cathodic partial current of H_2 was investigated [Figure 2(b)]. Increasing the catalyst loadings increased the cathodic partial current of product, especially at 1.5 and 2.0 mg/cm^2 loadings. The cathodic partial current of H_2 increased and became a constant value after –1.5 V vs.Ag/AgCl and when catalyst loadings were 0.5 and 1.0 mg/cm^2.

3.3 Kinetic analysis

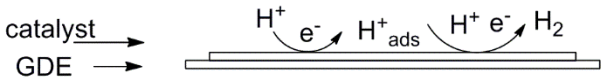

Scheme 1. The possible reaction pathway for HER on Cu(core)/CuO(shell) catalyst.

The HER process may be described by the differential equation:

$$\frac{d[H_2]}{dt} = k[H^+]^2 \qquad (1)$$

where t is the reaction time and k is the H_2 reaction rate constant.

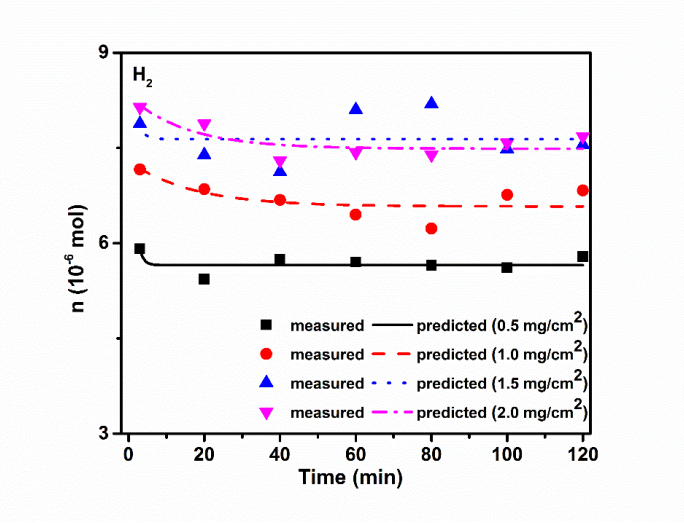

Figure 3. Comparison of experimental results with predicted moles for H_2 based on the differential model. Lines are predicted based on simulated differential model, dots are experimental data. Experimental conditions: working electrode = Cu(core)/CuO(shell) loading on GDE, counter electrode = Pt black loading on GDE, reference electrode = Ag/AgCl (3 M NaCl), solution is 1 M $KHCO_3$, at room temperature.

Based on the experimental results, we investigated in detail the HER on the Cu(core)/CuO(shell) catalyst during extended reduction reaction. Scheme 1 shows the proposed HER pathway during the CO_2 electrochemical reduction in the presence of the Cu(core)/CuO(shell) catalyst in 1 M $KHCO_3$.

Figure 3 shows the comparison of the product formation profiles between the proposed models and the experimental data. The results indicated that theoretical concentration values (in moles) of H_2 at different catalysts loadings were consistent with the experimental data. The model fitted well with the experimental data. The results, as presented in Figure 3**,** showed that the amount of H_2 decreased in the first 20 min and then reached a constant value during the rest of the reaction time. Notably, the measured H_2 value increased with increasing catalyst loadings during extended reduction. When the catalyst loadings were 1.5 and 2.0 mg/cm^2, the H_2 concentration was closed. This result indicated that H_2 evolution was not influenced by increasing catalyst loadings during extended reaction. The results demonstrated that the proposed differential model was fit for the HER. An increase in reaction time did not affect HER.

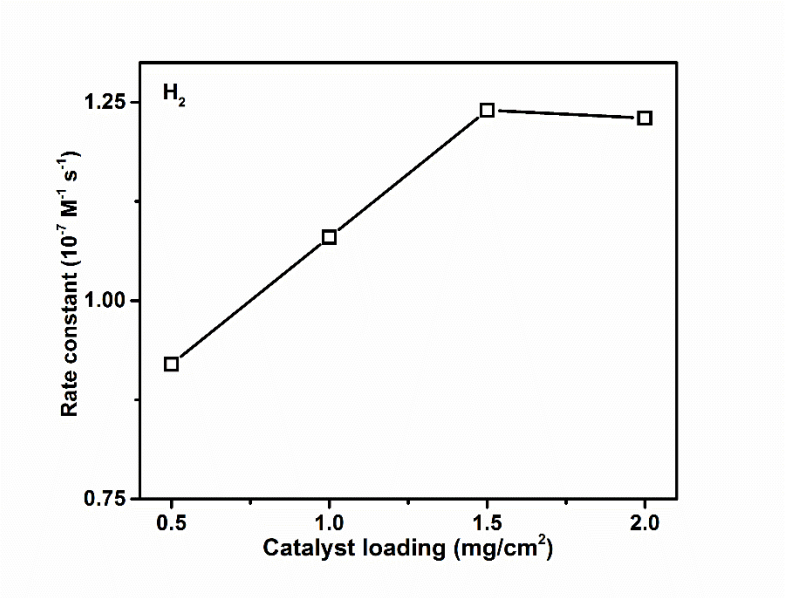

Figure 4. The rate constants of H_2 during the process of electroreduction of CO_2 on different Cu(core)/CuO(shell) loadings in a flow reactor in 1 M $KHCO_3$ at room temperature.

During electrochemical reactions, HER always occurred with CO_2 reduction. Therefore, it was necessary to understand the H_2 reaction kinetic constant to provide an insight into the effect of different catalyst loadings on H_2 evolution during electrochemical reduction. Figure 4 shows the H_2 rate constant as a function of catalyst loadings. The rate constant was calculated using the differential equations for *k*. Interestingly, *k* was affected by increasing catalyst loadings, but *k* was a constant value when the catalyst loadings were 1.5 and 2.0 mg/cm^2. This result explained the variation tendency of H_2 in an extended reaction.

4. CONCLUSION

The electrochemical behavior of the Cu(core)/CuO(shell) catalyst showed that the catalyst underwent conversions between various Cu oxidation states, namely Cu, Cu(I), and Cu(II). Chronoamperometric electrolysis was performed in a flow reactor to investigate the effect of catalyst loadings on the HER during the electrochemical reduction of CO_2. Increasing the catalyst loadings increased the H_2 Faradaic efficiency. The H_2 Faradaic efficiency became smaller when the cathode potential shifted to more negative values. The H_2 Faradaic efficiency of was between 40% and 65%. The HER pathway was proposed, and the differential equations deduced from the models were compared with experimental results. The use of the models described the evolution of products during electrochemical reaction. The H_2 rate constant indicated that H_2 evolution was affected by an increase in catalyst loadings. During the extended reaction, different catalyst loadings affected the electrochemical reduction of CO_2. This aspect will be investigated in a future study. The results suggested that the interactions between the Cu core and the CuO shell were beneficial for CO_2 and HER. These processes will be beneficial in future alternative energy studies.

ACKNOWLEDGEMENTS
We gratefully acknowledge the financial support from the International Institute of Carbon Neutral Energy Research (WPI-I2CNER), sponsored by the World Premier International Research Center Initiative (WPI), MEXT, Japan. The study was financed by the National Natural Science Foundation of China (21173085) and a China Council Scholarship awarded to Yangchun Lan.

References

1. A. J. Bard and M. A. Fox, *Acc. Chem. Res.*, 28 (1995) 141.
2. N. S. Lewis and D. G. Nocera, *Proc. Natl. Acad. Sci*., 103 (2006) 15729.
3. Y. Liang, Y. Li, H. Wang, J. Zhou, J. Wang, T. Regier and H. Dai, *Nature Mater*., 10 (2011) 780.
4. P. S. Fernández, E. B. Castro, S. G. Real and M. E. Martins, *Int. J. hydrogen energy*, 34 (2009) 8115.
5. J. Kubisztal, A. Budniok and A. Lasia, *Int. J. Hydrogen Energy*, 32 (2007) 1211.
6. A. W. Jeremiasse, J. Bergsma, J. M. Kleijn, M. Saakes, C. J. N. Buisman, M. C. Stuart and H. V. M. Hamelers, *Int. J. Hydrogen Energy*, 36 (2011) 10482.
7. C. Lupi, A. Dell'Era and M. Pasquali, *Int. J. hydrogen energy*, 39 (2014) 1932.
8. I. Ganesh, *Renewable and Sustainable Energy Review*, 31 (2014) 221.
9. H. Wang, L. X. Wu, J. Q. Zhao, R. N. Li, A. J. Zhang, H. Kajiura, Y. M. Li and J. X. Lu, *Greenhouse Gas Sci. Technol*., 2 (2012) 59.
10. C. J. Liu, *Greenhouse Gas Sci. Technol*., 2 (2012) 75.
11. H. Wang, L.-X.Wu, Y.-C. Lan, J.-Q. Zhao and J.-X. Lu, *Int. J. Electrochem. Sci*., 6 (2011) 4218.
12. M. Gattrell, N. Gupta and A. Co, *J. Electroanal. Chem*., 594 (2006) 1.
13. K. P. Kuhl, E. R. Cave, D. N. Abramc and T. F. Jaramillo, *Energy Environ. Sci*., 5 (2012) 7050.
14. J. Xiao, A. Kuc, T. Frauenheim and T. Heine, *J. Mater. Chem. A*, 2 (2014) 4885.
15. Y. Hori, Electrochemical CO_2 Reduction on Metal Electrodes, in: C. Vayenas, R. White, M. Gamboa-Aldeco (Eds.) *Modern Aspects of Electrochemistry*, vol. 42, Springer New York, 2008, Ch. 3, pp. 89.
16. D. T. Whipple and P. J. A. Kenis, *J. Phys. Chem. Lett*., 1 (2010) 3451.

17. Y. Hori, H. Wakebe, T. Tsukamoto and O. Koga, *Electrochim. Acta*, 39 (1994) 1833.
18. S. Ma, Y. Lan, G. M. J. Perez, S. Moniri and P. J. A. Kenis, *ChemSusChem*, 7 (2014) 866.
19. C. Graves, S. D. Ebbesen, M. Mogensen and K. S. Lackner, *Renewable and Sustainable Energy Reviews*, 15 (2011) 1.
20. Y. Hori, K. Kikuchi and S. Suzuki, *Chem. Lett*., (1985) 1695.
21. S. Kaneco, Y. Ueno, H. Katsumata, T. Suzuki and K. Ohta, *Chem. Eng. J*., 119 (2006) 107.
22. S. Kaneco, K. Iiba, H. Katsumata, T. Suzuki and K. Ohta, *Chem. Eng. J*., 128 (2007) 47.
23. A. A. Peterson, F. Abild-Pedersen, F. studt, J. Rossmeisl and J. K. Nørskov, *Energy Environ. Sci*., 3 (2010) 1311.
24. X. Nie, M. R. Esopi, M. J. Janik and A. Asthagiri, *Angew. Chem. Int. Ed*., 52 (2013) 2459.
25. D. Mignard, M. Sahibzada, J. M. Duthie and H. W. Whittington, *Int. J. Hydrogen Energy*, 28 (2003) 455.
26. X. An, J. Li, Y. Zuo, Q. Zhang, D. Wang and J. Wang, *Catal. Lett*., 118 (2007) 264.
27. S. Somasundaram, C. R. N. Chenthamarakshan, N. R. de Tacconi and K. Rajeshwar, *Int. J.Hydrogen Energy*, 32 (2007) 4661.
28. A. Paracchino, V. Laporte, K. Sivula, M. Grätzel and E. Thimsen, *Nature Mater*., 10 (2011) 456.
29. A. Paracchino, J. C. Brauer, J.-E. Moser, E. Thimsen and M. Graetzel, *J. Phys. Chem.C*, 116 (2012) 7341.
30. Z. Zhang and P. Wang, *J. Mater.Chem*., 22 (2012) 2456.
31. D. T. Whipple, E. C. Finke and P. J. A. Kenis, *Electrochem. Solid-State Lett*., 13 (2010) B109.
32. C. E. Tornow, M. R. Thorson, S. Ma, A. A. Gewirth and P. J. A. Kenis, *J. Am. Chem. Soc*., 134 (2012) 19520.
33. M. R. Thorson, K. I. Siil and P. J. A. Kenis, *J. Electrochem. Soc*., 160 (2013) F69.
34. E. J. Dufek, T. E. Lister and M. E. McIlwain, *Electrochem. Solid-State Lett*., 15 (2012) B48.
35. E. J. Dufek, T. E. Lister, S. G. Stone and M. E. McIlwain, *J. Electrochem. Soc*., 159 (2012) F514.
36. C. E. Tornow, M. R. Thorson, S. Ma, A. A. Gewirth and P. J. A. Kenis, *J. Am. Chem. Soc*., 134 (2012) 19520.
37. W. Z. Teo, A. Ambrosi and M. Pumera, *Electrochem. Commun*., 28 (2013) 51.